We are IntechOpen,
the world's leading publisher of
Open Access books
Built by scientists, for scientists

**4,800**

Open access books available

**122,000**

International authors and editors

**135M**

Downloads

Our authors are among the

**154**

Countries delivered to

**TOP 1%**

most cited scientists

**12.2%**

Contributors from top 500 universities

CLARIVATE ANALYTICS
**BOOK CITATION INDEX**
INDEXED

**WEB OF SCIENCE**™

Selection of our books indexed in the Book Citation Index
in Web of Science™ Core Collection (BKCI)

Interested in publishing with us?
Contact book.department@intechopen.com

Numbers displayed above are based on latest data collected.
For more information visit www.intechopen.com

# Barium Titanate-Based Materials – a Window of Application Opportunities

Daniel Popovici[1], Masanori Okuyama[2] and Jun Akedo[1]
*[1]National Institute of Advanced Industrial Science and Technology,*
*[2]Osaka University*
*Japan*

## 1. Introduction

Since it was discovered in 1945, barium titanate (BT) attracted much attention to researchers, becoming one of the most investigated ferroelectric materials due to good electrical properties at room temperature, mechanical and chemical stability and the easiness in its preparation. It is known that above the Curie temperature, the crystalline barium titanate has a cubic, perovskite-like structure as shown in figure 1.
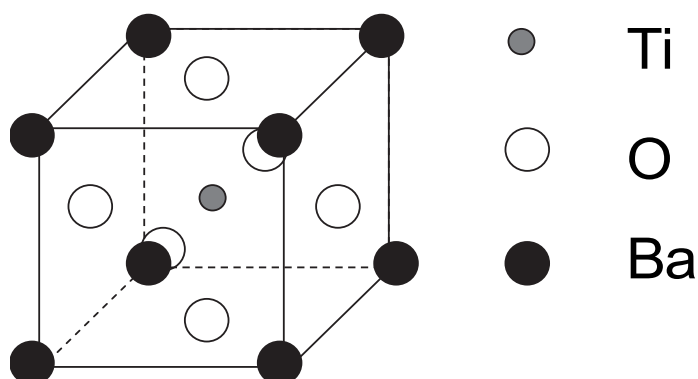


Fig. 1. Crystalline structure of BT material above Curie temperature

Below the Curie temperature, the crystalline cell is suffering a series of changes: to tetragonal (at $120^0$C), from tetragonal to orthorhombic (at $0^0$C) and from orthorhombic to rhombohedral (at $-90^0$C) in which the material has ferroelectric properties.

Theories concerning the ferroelectric behavior of crystalline materials that have a perovskite structure pinpoint the important role played by the spatial oxygen arrangement having an ion in its center, to the ferroelectrical properties. Taking this into consideration it is easy to predict that a change in spatial alignment of the oxygen octahedra or a substitution of the central ion (B-site substitution) can modify the ferroelectric behavior of the material. Change in spatial alignment of the oxygen octahedra can be also made by (so called) A-site substitution, when an A-site ion is substituted with another ion. In the case of barium titanate, it has been found that substitutions can make the temperature of paraelectric to ferroelectric transition to shift towards lower or higher values and, in some conditions, the

temperature of dielectric constant maxima will be affected by the frequency of the applied field (relaxor behavior). An A-site substitution, for example substituting $Ba^{2+}$ with $Sr^{2+}$ or $Pb^{2+}$, is responsible for shifting the temperature region in which the ferroelectric properties are present while the values of permittivity remain relatively large. This is good from the applications viewpoint because the possibility of shifting Curie temperature and the selection of the sector for the temperature dependence for dielectric constant and dielectric loss broadens the application area of these BT-based materials. The representative material in this class is $(Ba_{1-x},Sr_x)TiO_3$ (BST), one of the most studied solid solution due to its stability and the wide range of possible applications that can use its electrical properties.

A B-site substitution is also responsible of changing the degree of ordering in the solid solution resulting in a shift of Curie temperature and the appearance of the relaxor behavior when the local ordering of B-sites will make it favorable. In this category there is no widely studied BT-based material because their properties were comparable to other ferroelectric materials such as lead zirconate titanate (PZT), pure barium titanate, lead titanate or even barium strontium titanate. However, it has been found that small amounts of $BaZrO_3$ or $BaHfO_3$ included in BT can make it a candidate material for pyroelectric sensor, having electrical characteristics superior of those of lead lanthanum zirconate titanate (PLZT) or BST, materials that were commonly used for such applications.

As mentioned earlier, $(Ba,Sr)TiO_3$ (BST) solid solutions are one of the most investigated ceramic materials because the shift of ferroelectric phase transition towards lower temperatures can easily be controlled by adjusting the Ba/Sr ratio while maintaining acceptable high dielectric constants coupled with good thermal stability. $Ba(Ti,Sn)O_3$ (BTS) solid solutions are another subclass of materials that can be used for specific application. For a given application, to achieve the desired properties in the BST or BTS system, compositional control should be considered along with the preparation method and/or deposition method in the final device structure.

From many applications that can incorporate BT-based materials, here only optimization for two applications will be discussed in detail: dielectric bolometer mode of infrared sensor and embedded multilayered capacitor structures. Since the requirements for ferroelectric materials suitable for dielectric bolometer mode of infrared sensor and embedded multilayered capacitor structures are different, a good selection of ferroelectric material and fabrication method is necessary to ensure high quality ceramic layers for these applications. As a result, BTS thin films have been fabricated using metal-organic decomposition method as a suitable process to ensure good quality films for dielectric bolometer mode of infrared sensing applications. In the case of films for embedded multilayered capacitor applications, since the target require a low temperature fabrication technique, BST thick films have been fabricated using a relatively new deposition technique called aerosol deposition method, developed at National Institute of Advanced Industrial Science and Technology by Dr. Akedo, one of the coauthors of this paper, a fabrication method that allows fabrication of thick and dense ceramic layers at room temperature.

## 2. Preparation and characterization of BTS thin films for dielectric bolometer mode of infraredd sensor applications

One important characteristic for a material to be suitable for dielectric bolometer (DB) mode of infrared sensor applications is to have a large *Temperature Coefficient of Dielectric constant* (TCD).

$$TCD = \frac{(\varepsilon_r(T_2) - \varepsilon_r(T_1))}{\frac{(\varepsilon_r(T_2) + (\varepsilon_r(T_1))}{2}} \cdot \frac{100}{T_2 - T_1} \tag{1}$$

From 1990, $Ba(Ti_{1-x},Sn_x)O_3$ solid solution captured the attention of the researchers because of his stable ferroelectric properties in the vicinity of the Curie point that makes it a good candidate for specific applications. Because it belongs to a class of ferroelectric materials that show a diffuse phase transition (DPT) who have promising properties behavior that can be used for various applications such as sensors, actuators or high permittivity dielectric devices, this solid solution captured the attention of many research groups as a suitable active material. Investigation made with bulk $Ba(Ti_{1-x},Sn_x)O_3$ samples revealed that, if $BaSnO_3$ content is 30% or more, the solid solutions of $Ba(Ti_{1-x},Sn_x)O_3$ have relaxor behavior (Mueller et al., 2004; Lu et al., 2004; Yasuda et al., 1996; Xiaoyong et al., 2003). Moreover, Yasuda and al. observed a deviation of the dielectric constant from the Curie-Weiss law (that is specific for relaxor ferroelectrics) even when $BaSnO_3$ content is between 10 and 20%, but only in a narrow temperature region above Curie point, and a relaxor behavior for samples in witch the $BaSnO_3$ content is above 20%.

More recently, some authors see in $Ba(Ti_{1-x},Sn_x)O_3$ a candidate to replace $(Ba,Sr)TiO_3$ in microwave applications (Lu et al., 2004; Jiwei et al., 2004). Jiwei et al. showed that, in some conditions, tunability of a metal-ferroelectric-metal (MFM) structure could be as high as 54% at an applied field of 200 kV/cm and a frequency of 1 MHz.

A more important indirect result has shown by Tsukada et al. where, from the dielectric constant versus temperature for a $Ba(Ti_{1-x},Sn_x)O_3$ ($BaSnO_3$ content of 15%) thin film with a thickness of 400 nm deposited by PLD on $Pt/Ti/SiO_2/Si$, a value close to 11% at $25^0C$ can be calculated.

## 2.1 Fabrication of BTS thin films by metal-organic decomposition process

In the processing of the thin films, the goal is not only to reduce the cost and time in fabrication process but, more important, is to optimize the film properties for specific applications. Metal-organic decomposition process (MOD) has some advantages in comparison with other widely used deposition techniques: precise control of stoichiometry, high homogeneity, large area of deposition and simple equipment and process flow. However, one of the biggest problems implying this technique is that is not possible to fabricate crystalline thin films with epitaxial or columnar structure and that the density of the material is lower than the one obtained by other technique. High quality films can still be obtained by this process comparing with other techniques and, along with the advantages offered by MOD convinced many researchers to use it in their investigations.

Liquid solution of BTS was prepared by mixing barium isopropoxide $[Ba[OCH(CH_3)_2]_2]$, titanium butoxide $[Ti[O(CH_2)_3CH_3]_4]$ tin isopropoxide $[Sn[OCH(CH_3)_2]_4]$ and 1-methoxy-2-propanol supplied by Toshima MGF. CO.LTD.

The $Ba(Ti_{0.85},Sn_{0.15})O_3$ (BTS) solution was deposited on $Pt(240nm)/Ti(60nm)/SiO_2(600nm)/Si$ substrates by spin-coating at 500 rpm for 5 seconds followed by another 20 seconds at 2200 rpm. This step was performed in enriched $N_2$ atmosphere (1-5 l/min flow) to avoid moisture, because the solution is highly hygroscopic. After spin coating, the film was moved quickly on a hot plate and dried at $250^0C$ for one minute followed by 10 minutes drying into an oven at the same temperature in air. After drying, the BTS films were pyrolyzed at $450^0C$ for 10 minutes into an oven in enriched $O_2$ atmosphere (1 l/min

Fig. 2. Process flow of the BTS thin films prepared by MOD



Fig. 3. TG-DTA analysis results of the BTS MOD-solution

flow). Spin-coating / drying / pyrolyzing sequence was repeated another 4 times before annealing in enriched $O_2$ atmosphere (1 l/min flow) for 10 minutes was performed. The BST15 thin films were annealed at 600⁰C, 700⁰C, 750⁰C or 800⁰C. The deposition and heat treatment were repeated 20 times before a final annealing was performed for 20 minutes in $O_2$ enriched atmosphere. The schematic representation of the deposition steps is shown in Figure 2. Differential thermal analysis (DTA) and thermo-gravimetric analysis (TG) (Figure 3) were used to determine the thermal decomposition behavior of the BTS solution and to select the appropriate temperatures for drying and baking. DTA curve shows an endothermic peak at 103⁰C corresponding to solvent evaporation point and two exothermic

peaks at 350 and 370$^0$C, temperatures that correspond to precursor decomposition and formation of BTS compound. The TG curve showed that the total mass of the investigated liquid decreases rapidly at the beginning, the solution loosing almost 94% of its mass at 180$^0$C and slowly loosing more, reaching -97% at 380$^0$C. The weight loss is insignificant above 380$^0$C.

According to TG-DTA results, a drying temperature over 180$^0$C and a baking temperature over 370$^0$C are necessary. A drying temperature of 250$^0$C and baking temperature of 450$^0$C were selected to ensure full solvent evaporation in short time and to minimize as much as possible the stress and defects caused by a further weight reduction during annealing and a rapid complete precursor decomposition and BTS formation.

The thickness of the BTS15 films obtained by this process was about 360nm.

After BTS thin films preparation was completed, Pt/Ti electrodes were formed on the film by RF sputtering to make BTS capacitors. After completion of BTS capacitor fabrication, for films annealed at 700$^0$C, a post electrode-forming annealing was performed at temperature varying from 200 to 350$^0$C in air and at 300$^0$C in high vacuum for 60 minutes.

In order to obtain high quality films suitable for DB-mode of infrared sensing applications (high values of TCD), the BTS thin film properties have been studied for different fabrication conditions and the results were used to optimize the deposition conditions for improved BTS thin films. The influence of annealing temperature and postannealing treatment on physical and electrical properties of the fabricated BTS thin films was investigated aiming an increase in TCD values near room temperature. The temperature of maximum permittivity for the fabricated BTS thin films was found to be near 13$^0$C.

## 2.2 Annealing and postannealing treatment effect on BTS thin film properties

The annealing effect on the properties of the fabricated BTS thin films has been checked first in order to optimize the fabrication conditions.
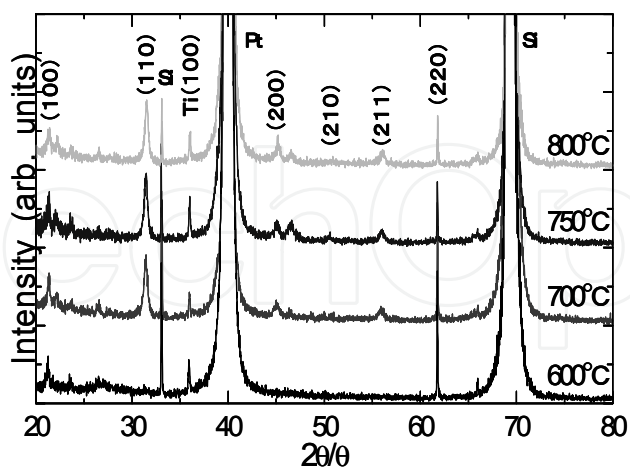


Fig. 4. XRD patterns of the BTS thin films annealed at different annealing temperatures

In Figure 4, XRD patterns of the films annealed at temperature ranging from 600$^0$C to 800$^0$C are showed. The films annealed at 600$^0$C are still amorphous but for films annealed at 700$^0$C and higher, crystal structure has been detected. The films have strong (110) peaks suggesting that the crystalline BTS films have a preferential orientation along (110)

direction. The other peaks, assignable to a cubic perovskite type structure, are also present but their intensities are much smaller than the intensity of (110) peak. The preferred orientation and intensity ratios among the peaks revealed little distinct differences among these films as a function of annealing temperature. The average grain size was estimated from the half-width of the x-ray diffraction peak using Scherrer's formula to be in the 33.3 – 50 nm range.

For films fabricated at annealing temperatures of 700, 750 and 800°C, leakage currents, C-V and temperature dependence of capacity (and through it, the permittivity dependence) were measured and analyzed. Except the temperature dependence of capacity, the other electrical measurements were performed at room temperature, well above the temperature of maximum permittivity.

The leakage current measurements showed that the films annealed at 750°C have a higher leakage current than films annealed at 700°C and 800°C (Figure 5). The reason for this behavior is still not clearly understood. Because films with small leakage currents are desired the films annealed at 750°C cannot be considered suitable for DB-mode infrared sensing applications. For this reason the attention was focused on the films annealed at 700°C and 800°C.
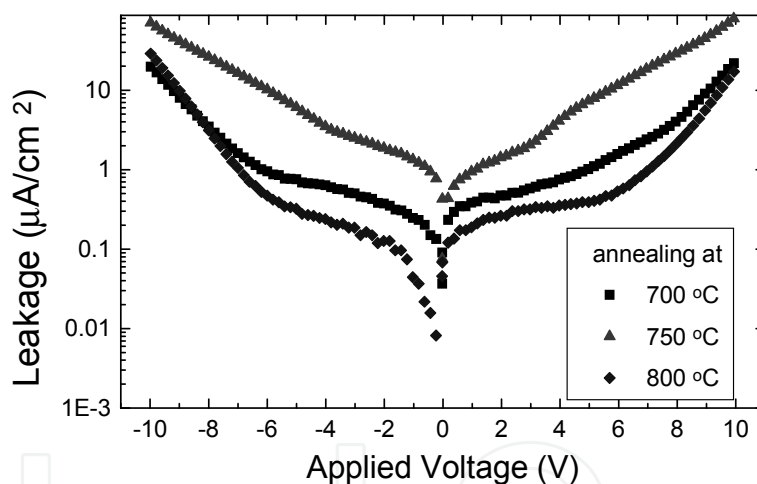


Fig. 5. Leakage current for BTS films annealed at different temperatures

The investigations of the temperature influence on the dielectric loss (Figure 6) revealed that the dielectric loss increases with increase in annealing temperature. Moreover, the dielectric loss for films annealed at 800°C shows large temperature dependence compared with films annealed at 700 and 750°C. On the other hand, the films annealed at 700°C have the dielectric loss very little affected by the increase in the annealing temperature.

In Figure 7, temperature dependence of capacitance for films annealed at 700°C and 800°C has been plotted. The variation of capacitance for BTS samples annealed at 700°C is more pronounced than for the samples annealed at 800°C.

Reviewing the results obtained after physical and electrical properties in becomes clear that annealing at 700°C is more suitable in obtaining BTS thin films with good properties for DB-mode of infrared sensor applications.
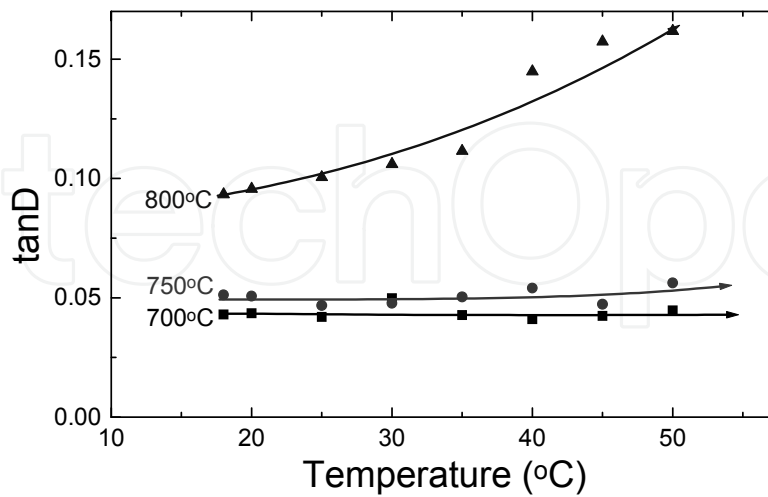
Fig. 6. Dielectric loss vs. sample temperature for BTS films annealed at different temperatures
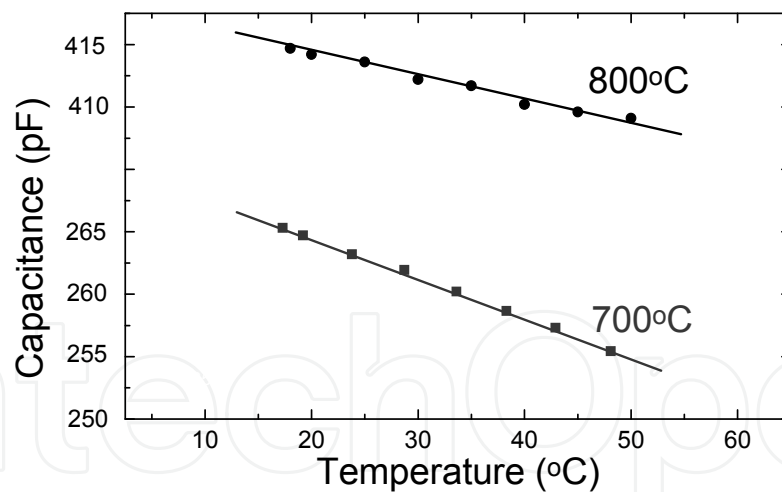


Fig. 7. Capacitance vs. sample temperature for BTS films annealed at 700°C and 800°C

The effect of postannealing temperatures on physical and electrical properties of BTS thin films was investigated keeping in mind that the films should be suitable for DB-mode of infrared sensor. The annealing temperature has been set to 700°C as a result of annealing temperature effect investigations performed earlier. After the top-electrode deposition, a postannealing treatment has been performed at temperatures of 200, 300 and 350°C in air and at 300°C, in vacuum for 60 minutes. The results of the investigations made on BTS samples are summarized in Table 2.

| postannealing | Leakage density | TCD (25ºC) | polarization | Grain size | Dielectric loss |
|---------------|-----------------|------------|--------------|------------|-----------------|
| not | $200\mu A/cm^2$ | 0.72-1 %/K | | | 0.04 |
| 200ºC | $1\mu A/cm^2$ | 1.3 %/K | | Not affected | 0.04 |
| 300ºC | $100\mu A/cm^2$ | 5.6 %/K | | | 0.06 |
| 350ºC | $100\mu A/cm^2$ | 1-1.1 %/K | | | 0.04 |

Table 2. Postannealing effect on physical and electrical characteristics of BTS thin films. Leakage densities are given for an applied voltage of 10V

Only some electrical properties are affected by the treatment. Polarization in P-E hysteresis loops is increasing with the increase in postannealing temperature (not shown here). This can be explained considering the fact that a postannealing treatment is improving the metal-ferroelectric interface. The effect of oxygen diffusion during postannealing treatment should not be neglected while considering improvement in polarization. However, as we will show below, increase in polarization due only to improvement in film surface due to reduction in oxygen vacancies by oxygen diffusion from air cannot fully explain the tendency.

Analyzing the results summarized in Table 2 it can be seen that the current leakage of the BTS samples is the most affected by postannealing temperature being smaller for films postannealed at 200ºC. It can be observed that increase in postannealing temperature will not further improve the leakage currents of the samples. Y. Fukuda et al. (Fukuda et al., 1997) reported that, by increasing the postannealing temperature in the case of $(Ba,Sr)TiO_3$ thin films deposited on $Pt/SiO_2/Si$ or $SrTiO_3$ substrates, the diffusion of the oxygen from the postannealing atmosphere is decreasing. Our results suggest the same effect by increasing the postannealing temperature because the leakage current, even if it is better than that for as-deposited samples, is increasing by increasing the annealing temperature.

Figure 8 is showing the $I-E^{1/2}$ characteristics of the leakage current for BTS samples postannealed at 200ºC and 350ºC along leakage current for samples that were not postannealed. The leakage behavior for samples postannealed at 300ºC is not shown to avoid overlay in the graphic because it shows almost the same behavior as samples annealed at 350ºC. It can be seen in the figure that postannealing treatment decreases Schottky leakage currents. The Schottky currents can be described by (Sze, 1981; Fukuda et al., 1998):

$$J = A^* T^2 \exp\left(-q\Phi_B / kT\right)\exp\left(q\alpha E_{\text{int}}^{1/2} / kT\right) \tag{2}$$

$$\alpha = \left(q / 4\pi\varepsilon_i\right)^{1/2} \tag{3}$$

where $A^*$ and $\Phi_B$ are the effective Richardson constant for electrode emission and the Schottky barrier height between cathode and the ferroelectric thin film, T is the temperature in Kelvin, $E_{\text{int}}$ is the electric field at the interface and $\varepsilon_i$ is the dynamic dielectric constant of the ferroelectric media.
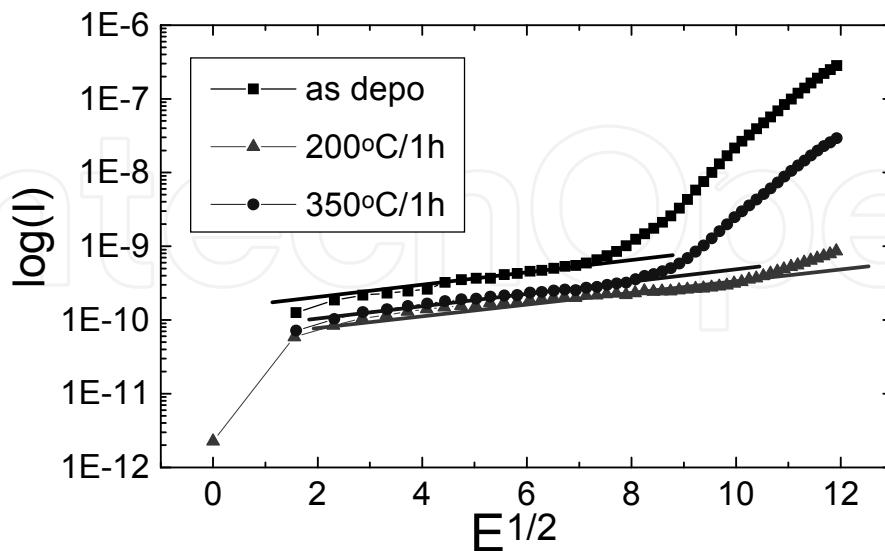
Fig. 8. J-$E^{1/2}$ characteristics of the leakage current for BTS samples, as-deposited and postannealed at $200^0C$ and $350^0C$ (Schottky currents)

In figure 8 it can be observed that the first part of the I-$E^{1/2}$ characteristics can be plotted with a straight line, suggesting that the leakage is mainly due to Schottky currents. Moreover, the plotted lines seem to be almost parallel to each other. Similar result has been obtained by Fukuda while investigating the effects of postannealing in oxygen ambient on leakage properties of $(Ba,Sr)TiO_3$ thin film capacitors (Fukuda et al., 1998). Because the plotted lines are parallel, all parameters except $\Phi_B$ in the equation (2) are almost equal in all cases. Increase in Schottky barrier and, thus, decrease in the leakage can be explained considering the oxygen that was diffused during postannealing treatment. Since, a correlation between the oxygen vacancy in the film and the diffusion coefficient can be made (Fukuda et al., 1997; Fukuda et al., 1998), an increase in the Schottky barrier can be explained by decrease in the oxygen vacancy concentration at the metal-ferroelectric film interface.

Focusing the attention back to table 2, it can be seen that TCD is highest for samples postannealed at $300^0C$ reaching 5.6% at $25^0C$. Even if the leakage behavior for samples postannealed at $300^0C$ and $350^0C$ is almost similar, we expect a difference in oxygen vacancy concentration due to different oxygen diffusion coefficients.

In order to understand how postannealing at $300^0C$ is improving the value of TCD, the postannealing treatment has been performed in air as well as in high vacuum conditions. In this way the effect of presence of oxygen in the postannealing atmosphere can be better understood. Physical and electrical properties (especially leakage current and TCD versus sample temperature) were again investigated but this time the attention has been focused into noticing any particular differences among samples.

Post-annealing after electrode deposition in air or vacuum was found to have little effect on the BTS XRD peaks, indicating that the crystalline structure is not changed after the post-annealing. AFM observation (not shown here) revealed a root-mean-square (RMS) roughness of 1 to 3 nm.

The chemical change induced by the postannealing in films was obtained after XPS investigations (Figure 9). The attention was focused upon the chemical shifts that were clearly visible in the samples. The peaks were carefully calibrated using the Pt peaks and viewing the carbon peaks for confirmation.
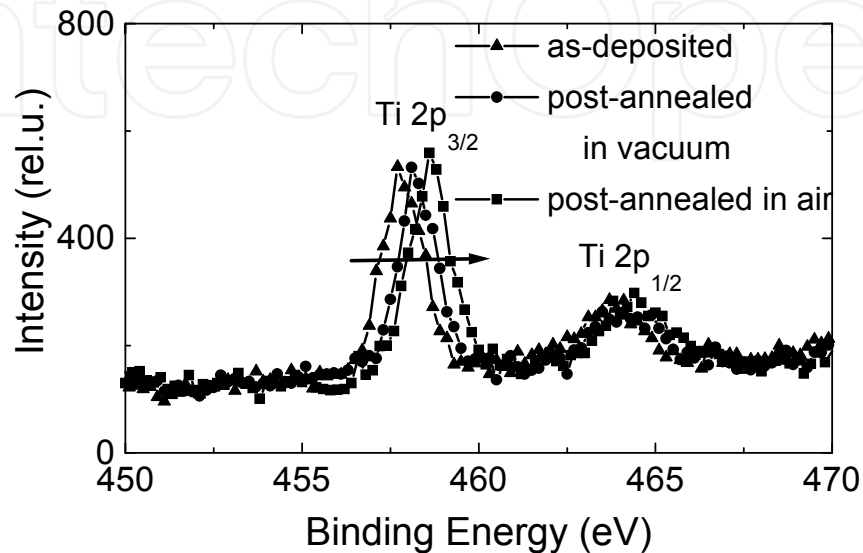


Fig. 9. XPS spectra for BTS thin films as-deposited and postannealed at 300ºC for 1 hour in vacuum and air.
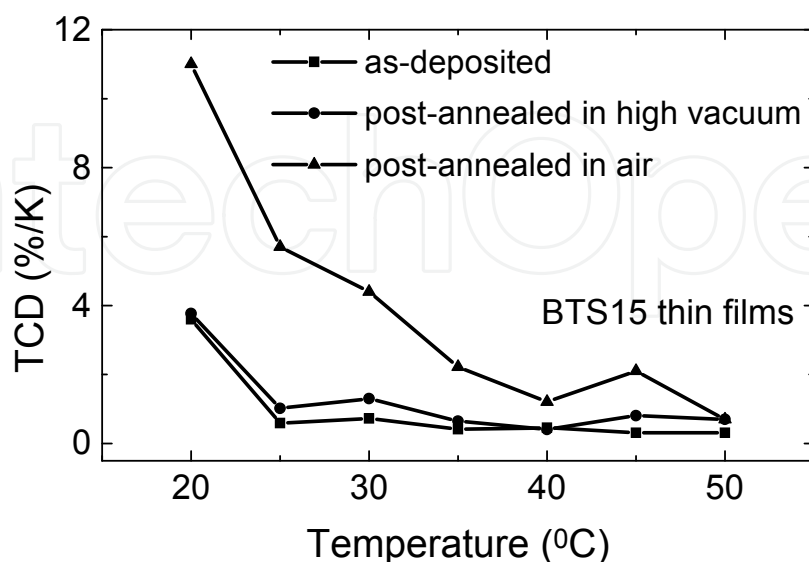


Fig. 10. TCD vs.film temperature for BTS thin films as-deposited and postannealed at 300ºC for 1 hour in vacuum and air

The exact binding energy of an electron depends upon the formal oxidation state of the atom from which it was extracted and local chemical and physical environment. The postannealing after electrode deposition was performed in air as well in vacuum to study the influence of diffused oxygen to the chemical properties of the near-surface layer of the BTS thin films. For postannealed films in vacuum or air, the Ti peaks are shifting towards higher binding energies than Ti peaks for as-deposited films. The presence of $O_2$ in the air can explain why the Ti peaks for the sample postannealed in air are shifting more than the Ti peaks for the sample postannealed in vacuum. Chemically speaking, the presence of $O_2$ in postannealing atmosphere causes oxygen diffusion into the BTS thin films that will be responsible for the reduction in concentration of the oxygen vacancies near the surface, increasing the oxidation state of the Ti, causing the shift of the Ti peaks position towards higher binding energies in XPS investigations.

An important electrical measurement is the investigation of the temperature dependence of the capacitance (i.e. dielectric constant). Figure 10 shows the TCD behavior for BTS thin films as-deposited and postannealed in air and vacuum. The films post-annealed at 300°C in air have TCD values reaching more than 5.4 %/K at 25°C and 11 %/K at 20°C, which is very high compared with similar reported values for TCD. The improvement in TCD values makes the BTS thin film very promising for realizing highly sensitive dielectric-bolometer mode of infrared sensor.

### 2.3 DB-mode of infrared sensor using BTS thin films as active materials

Because of the principle of operation, a dielectric-bolometer mode is expected to offer high sensitivity compared with other detectors (Noda et al., 1999; Balcerak, 1999; Radford et al., 1999; Noda et al., 1999). This aspect, along with other advantages offered, such as chopper free device and low operation voltages are good reasons to consider the DB-mode a good choice in fabricating an infrared sensor.

Following the results obtained for ferroelectric BTS thin films, integration into a simple infrared sensing structure will confirm that the BTS can be considered a good candidate for DB-mode of infrared sensing applications.
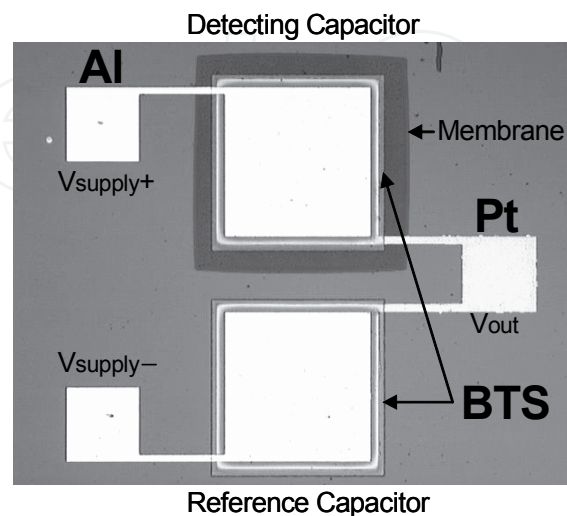


Fig. 11. Picture view of the infrared sensor cell

In order to investigate what are the sensor capabilities of a structure containing BTS thin film as detecting layer, a simple structure was made, containing a simple capacitance ratio sensor that will sense any capacitance difference between detector and reference capacitors. A picture view of the fabricated structure is shown in Figure11.

Fabrication of the structure on silicon was made with the use of silicon micro machining process. The fabrication steps are shown in Figure 12. Only the detector-capacitor is constructed on a membrane, the reference capacitor will stay on $SiO_2/Si_3N_4/SiO_2/Si$ substrate.
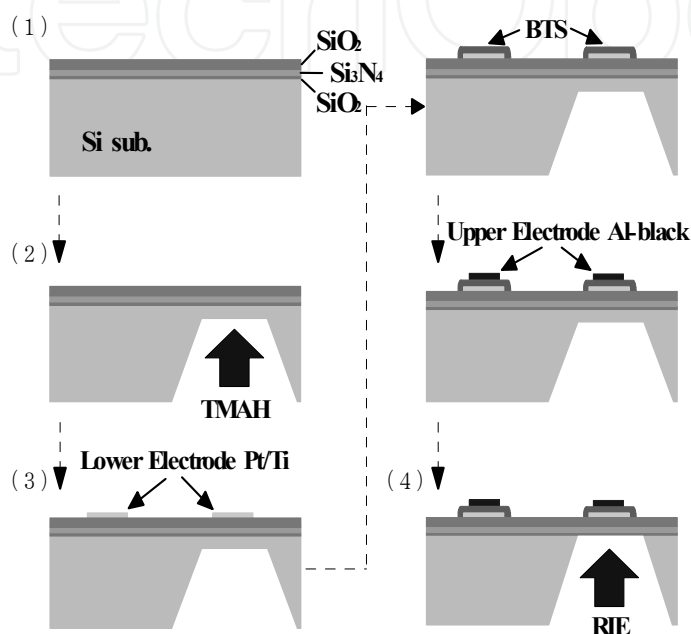


Fig. 12. Process of infrared sensor fabrication
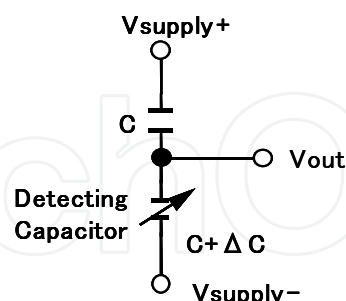


Fig. 13. Detection circuit for infrared measurement

Schematically, an infrared sensing cell can be represented as in Figure 13. A sensing cell is composed of serially connected capacitors. This sensor cell is operating on the principle of sensing the change in the capacitance of the detector-capacitance relative to reference capacitance. Because of the construction, when the sensing cell is exposed to infrared radiation, the temperature at the ferroelectric BTS material site for the detecting capacitor is higher compared with the one for the reference capacitor. Different temperatures are responsible for different dielectric constant values at the detector and reference capacitors

that translate into different capacitance values. The variation of the capacitance of the detector-capacitor relative to the value of the capacitance in reference capacitor is detected as a voltage change. Because this voltage signal is very small, amplification is required for the detection.

The infrared response evaluation system is showed schematically in Figure 14. In infrared response evaluation, the temperature of a black body radiator (600$^0$C to room temperature range) is used as source of infrared rays. The infrared rays were focused with germanium lens so that the radiation will fall mainly on the single element sensor. A function generator was used to apply sinusoidal waves with voltage amplitude of 3V, offset of 1.5V and frequency of 1kHz to both capacitors. An almost 180 degree reversal of the phase was used in the capacitors in order to minimize the output signal. When infrared radiation will fall on the detecting capacitor, heating will cause a change in the value of capacitance. This change will affect the "equilibrium" state in the circuit and a $V_{out}$ signal will be detected. The output voltage is then amplified through the band-pass filter of 1 kHz for which lock-in amplifier was substituted and observed as an output waveform with an oscilloscope. Furthermore, using the high-speed Fourier transform (FFT) function built in the oscilloscope, the output signal is extracted.
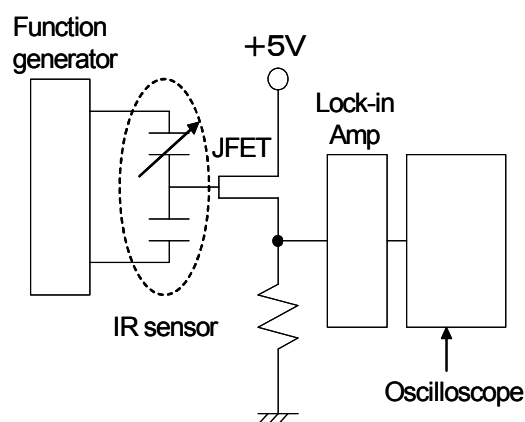


Fig. 14. Infrared response evaluation system

The optimization of the DB operation conditions has to be made before making any comment about the sensing properties of the ferroelectric BTS thin films. Running a set of experiments such as DB output voltage behavior at different applied voltages considering the low leakage behavior of the films at low applied voltages or DB output voltage behavior at different applied frequencies are essential in increasing device sensitivity.

Blackbody temperature dependence of DB output as a parameter of the operation amplitude of supply voltage is showed in Figure 15. For the same sensing cell structure and the same applied frequency, DB output signal is increased by increase in applied voltage amplitude.

Blackbody temperature dependence of DB output as a parameter of the applied frequency of supply voltage is shown in Figure 16.

It can be seen that the DB output level increases with decreasing the frequency of the supplied voltage. The reason for this behavior is considered to be the fact that not the entire voltage amplitude is applied to the series capacitor structure while the frequency is increased.

It can be concluded now that the optimal DB operation conditions are:

1. Larger amplitude of supply voltage. The amplitude should be, however, small enough to ensure small leakage currents through the BTS thin film. 3 to 5 V amplitude for the applied voltage is considered here;
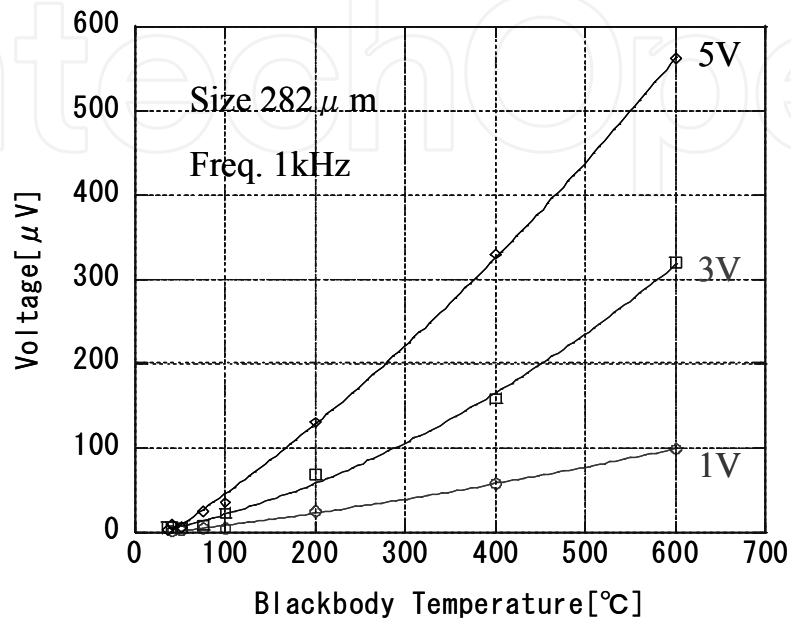2. Low operation frequency for the applied voltage. 10 or 100Hz is considered in this experiment.

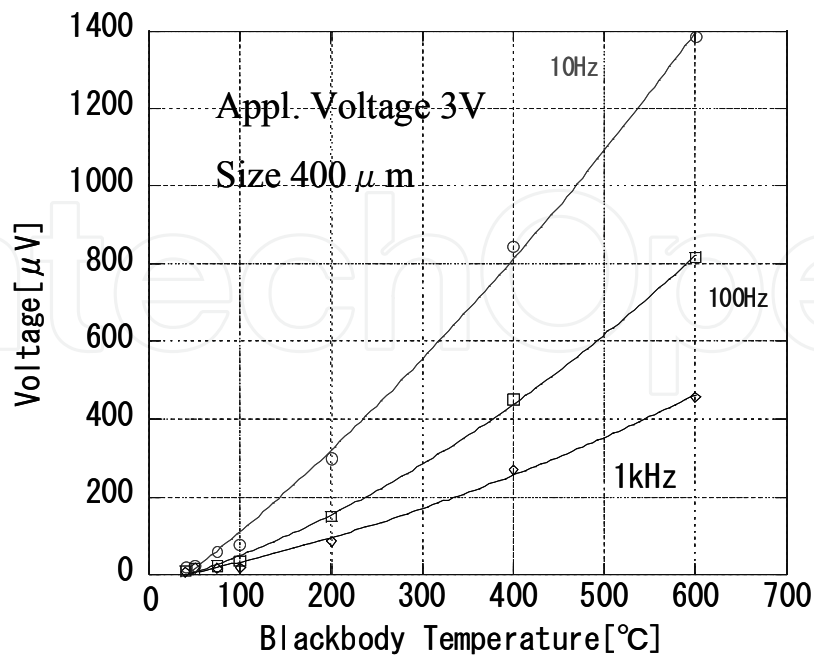Fig. 15. DB output as a parameter of the operation amplitude of supply voltage

Fig. 16. DB output as a parameter of the operation frequency of supply voltage

As a result of optimization, sensing properties of the BTS ferroelectric thin film can be investigated. The output voltage for infrared sensing cells containing BTS thin films as deposited and postannealed at 300⁰C in air for 60 minutes is shown in Figure 17.
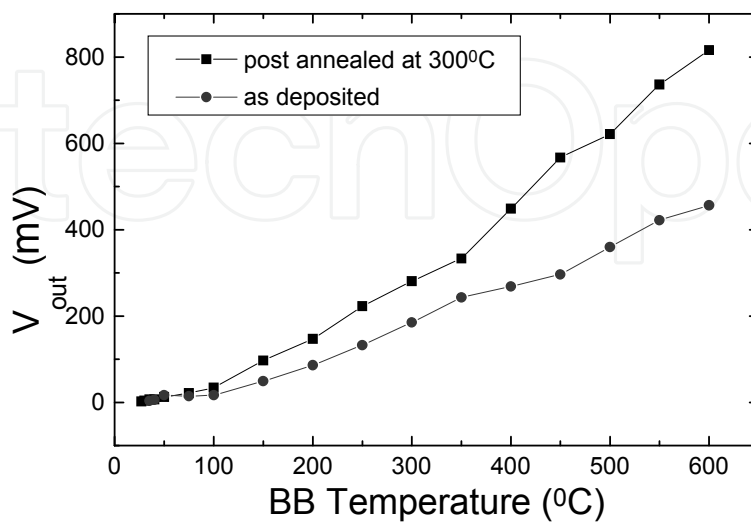


Fig. 17. Output voltage vs. blackbody temperature for sensing cells containing BTS thin films as deposited and postannealed at 300⁰C in air
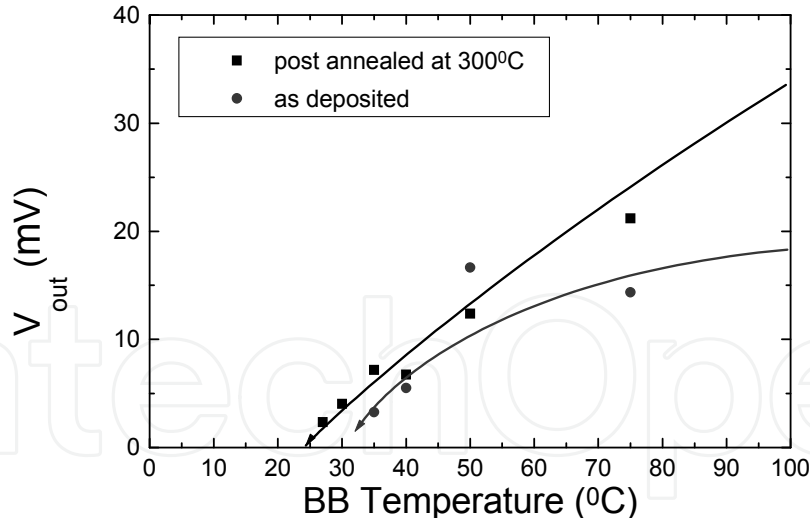


Fig. 18. Output voltage for blackbody temperatures below 100⁰C for sensing cells containing BTS thin films as deposited and postannealed at 300⁰C in air

The importance of postannealing can be clearly seen from this figure. Moreover, a closer look at the response while exposing to the infrared radiations emitted by the black body when its temperature was below 100⁰C (Figure 18) revealed that a stable detection of infrared radiation emitted by a blackbody when its temperature was 27⁰C was successfully obtained. However the output signal is less than expected because 75% of the incident

radiation is reflected by the top electrode; only a maximum of 25% of incident radiation will cause the heating in the sensing cell. Voltage responsivity ($Rv$) and specific detectivity ($D^*$) were calculated to be 0.1 KV/W and $3 \times 10^8$ cmHz$^{1/2}$W, respectively, being in the same range as thin metal oxide film bolometers.

BTS obtained by metal-organic decomposition process can be successfully used as active material in fabrication of DB-mode of infrared sensor. As demonstrated above, temperatures lower than the temperature of a human body can be successfully detected by this type of infrared sensor cell using BTS deposited by metal-organic decomposition process as active material.

## 3. Preparation and characterization of (Ba$_{0.6}$,Sr$_{0.4}$)TiO$_3$ thick films for application to embedded multilayered capacitor structures

The demand of miniaturization and increased functionality in electronic devices triggered the need of finding ways to increase densification of components on electronic boards and 3D packing. There is a need to improve current technologies or develop new ones in order to cope with the problems that arise with miniaturization and 3D packing. The use of high temperatures during fabrication are not desirable since can trigger unwanted chemical reactions, interdiffusion, shrinkage and/or alteration of electrical properties for the component already present on the circuit board. A relatively new deposition method called the Aerosol Deposition (AD) technique based on room temperature impact consolidation (RTIC) phenomena can be a good alternative in film formation at room temperature (Akedo & Lebedev, 1999; Akedo et al., 1999; Akedo & Lebedev, 2001; Akedo, 2004; Akedo, 2006). In this way, the problems linked with relatively high temperatures needed for film formation using the current (more popular) technologies can be avoided and embedding of dense ceramics into low temperature substrate becomes possible.

As mentioned earlier, barium strontium titanate is an extensively investigated ferroelectric material due to its good electrical properties in bulk and thin film form being a leading candidate for applications in many electronic devices. Barium strontium titanate is currently considered as an attractive material in sensing, memory, capacitor and RF and microwave applications (Kirchoefer et al., 2002; Acikel et al., 2002; Hwang et al., 1995; Zhu et al., 2004; Tissot, 2003). But many important issues, such as improving dielectric constant values, dielectric loss and leakage, still need further attention in order to improve film quality and device performance. Regarding the AD-deposited (Ba$_{0.6}$,Sr$_{0.4}$)TiO$_3$ (BST) films, there are few reports regarding the film particularities. The logical ways to improve film properties are by tempering with film chemical composition, deposition conditions and post-film-formation treatments, and metallization. However, preliminary results have shown that post-film formation annealing is not helpful to improve the properties of the AD-fabricated BST films (Popovici et al., 2009). The substrate is also playing an important role in improving the AD-fabricated BST film properties since a soft substrate is suitable in ensuring that the films are less stressed (Popovici et al., 2008).

For AD process, powder condition is one of the most important factors since humidity, physical characteristics of the particle and particle aggregation are affecting the deposition rate and film properties.

Below, only the results on the investigation regarding the quality of commercially available (raw) powder used in the AD-deposition and improvement by heat treatments to allow the

fabrication of $(Ba_{0.6}, Sr_{0.4})TiO_3$ (BST60) layers with higher dielectric constants will be discussed due to space constrains in writing this article.

### 3.1 Aerosol Deposition method as alternative technique in BST thick film deposition

BST60 thick films were grown by the AD technique on Cu substrates using raw and thermally treated powders. To investigate the effect of powder thermal treatment on AD-fabricated BST60 thick films properties, powder from the same lot has been thermally treated for 1 h at 800 or $900^0C$ in $O_2$ atmosphere.

The AD system used in film fabrication is represented schematically in figure 19. Powder aerosols are formed by oxygen flowing in the vacuum powder chamber at a rate of 4 l/min and transported through connecting tubes to the vacuum deposition chamber where the particle are ejected through the nozzle toward a moving substrate for deposition. A schematic representation of the consolidation process by AD is shown in figure 20. During AD deposition, the particles will suffer a plastic like deformation and fracture upon impact with the substrate. This plastic like deformation and the fracture of the impacting particles are essential to ensure the formation of very dense AD films.
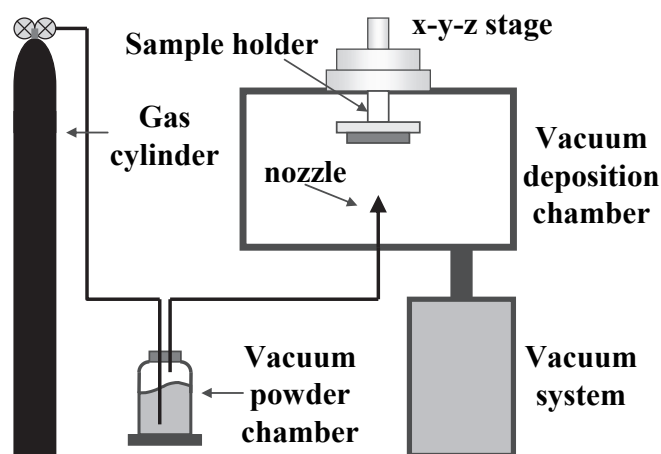


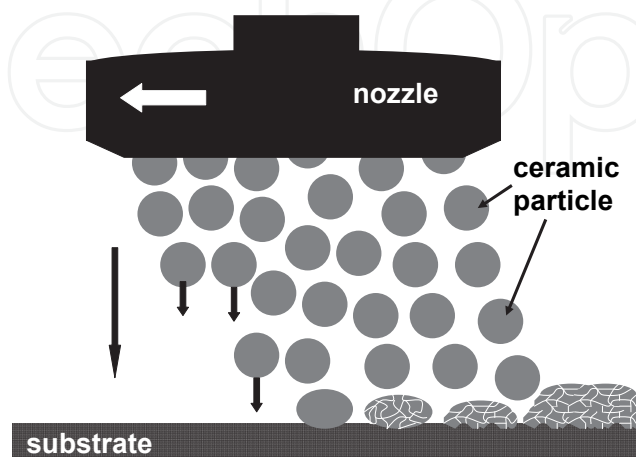Fig. 19. Schematic representation of AD system



Fig. 20. Schematics of consolidation process by AD

Before being used in AD, the powder is optimized by ball milling to allow fabrication of high quality films at high deposition rates and with minimum consumption of powder. The average particle size after ball milling should fall within the optimum range (considered to be 0.7-1.4 µm for the BST powder). The thickness of the fabricated BST60 films was around 3 µm and their density was estimated to be in the 92-93% range from the theoretical density, being independent of the powder condition. To examine the electrical properties of the films, Pt/Ti electrodes were deposited by RF sputtering on BST60 thick films to form capacitor structures.

## 3.2 AD-fabricated BST thick film properties

In BST powder synthesis, there are a number of reports that suggest that the presence of $BaCO_3$ in BT and BST powders is difficult to prevent whatever the fabrication route is used (Henningh & Mayr, 1978; Coutures et al., 1992; Hennings & Schreinemacher, 1992; Stockenhuber et al., 1993; Lemoine et al., 1994; Ries et al.,2003). Moreover, there are reports that suggest that BT is thermodynamically unstable in $H_2O$ having a pH below 12 (Lencka & Riman, 1993; Abicht et al., 1997; Voltzke et al.,1999). The BST is expected to show a similar problem since it is a BT-based material. The most probable chemical reaction with water is shown below:

$$BaTiO_3(s)+9H_2O \rightarrow Ba(OH)_2+8H_2O+TiO_2(s). \tag{4}$$
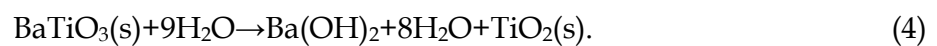
The formed solid $TiO_2$ (amorphous) will remain in the outer shell of the initial BT (or BST) particle and will act as a barrier in the further removal of Ba by water (Voltzke et al., 1999). Upon air exposure, $Ba(OH)_2$ will react as follows:

$$Ba(OH)_2+CO_2(air) \rightarrow BaCO_3(s)+H_2O \tag{5}$$
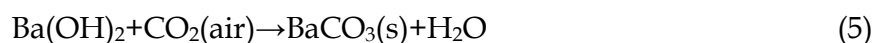
The instability of strontium titanate (STO) material in water is not confirmed, therefore, only, only the instability of $Ba^{2+}$ ions in $H_2O$ is considered here.

Whatever the reasons for the presence of $BaCO_3$ as a secondary phase in BST and BT powders, $BaCO_3$ formation must be controlled to ensure the fabrication of BST or BT films with the desired properties since AD is a room temperature process and post-film-formation thermal treatments at elevated temperatures are not reccomended.

X-ray photoelectron spectroscopy (XPS) has been used to clarify the presence of the secondary phase in the powder and films and the effect of powder annealing. The powder specimens were prepared on Al plate using a commercial double-sided adhesive tape on which the powder adhered. The tape was well covered with powder to avoid the occurrence of tape-related peaks in the XPS spectra. For calibration purpose and to avoid charging due to electron photoemission, a very thin layer of Au was deposited on the surface of the samples by RF sputtering. Six elements were detected on the surface of the investigated samples: C, Au, O, Ba, Sr and Ti. The Au peaks were used to calibrate the XPS profiles.

The XPS profiles of the C 1s peaks of raw powder, the AD-fabricated film obtained from this powder, and powder recovered from the deposition chamber are shown in figure 21. The C 1s peak located near 284.8 eV is commonly attributed to C-C and C-H bonds. The C 1s peak located near 288.45 eV is assumed to be correlated with the C state in $CO_3^{2-}$ of $BaCO_3$ (Viviani et al, 1999) since the other possible chemical states for carbon, C-O and $CO_2$, should reveal peaks located at binding energies that are higher with approximately 2 eV (Viviani et
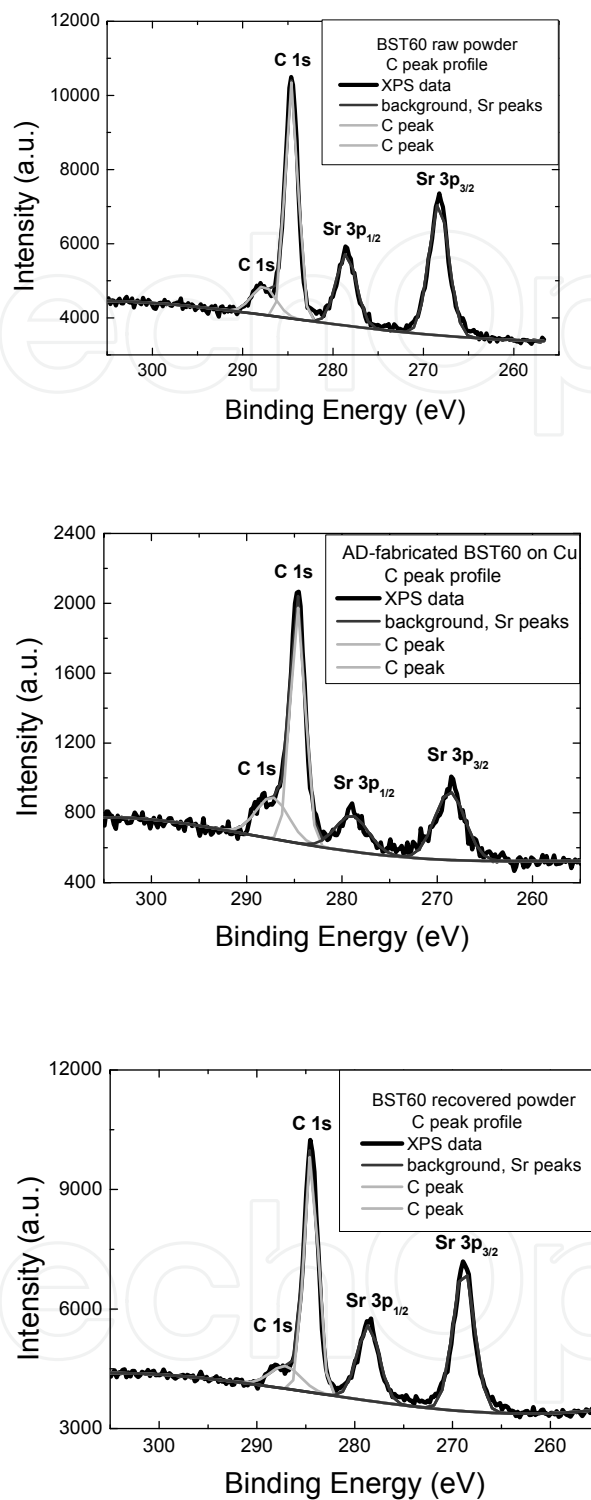
Fig. 21. XPS C1s peak profile for raw and annealed powders

al, 1999) and 7 eV (Wagner et al.,1979), respectively, than those of the reference C 1s peak. Comparing the relative intensities of the $CO_3^{2-}$-related C 1s peak (relative to Sr $3p_{3/2}$ peak) for the raw powder, AD-fabricated BST60 film, and powder recovered from the deposition chamber it can be concluded that the relative intensity of the carbonate phase is higher in the AD-fabricated film than in the powder.
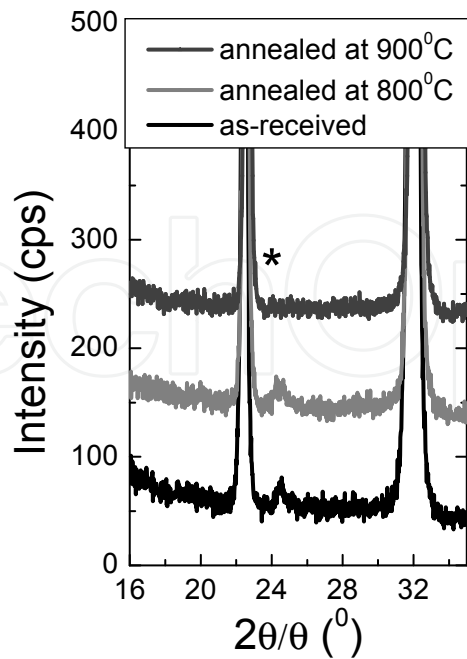
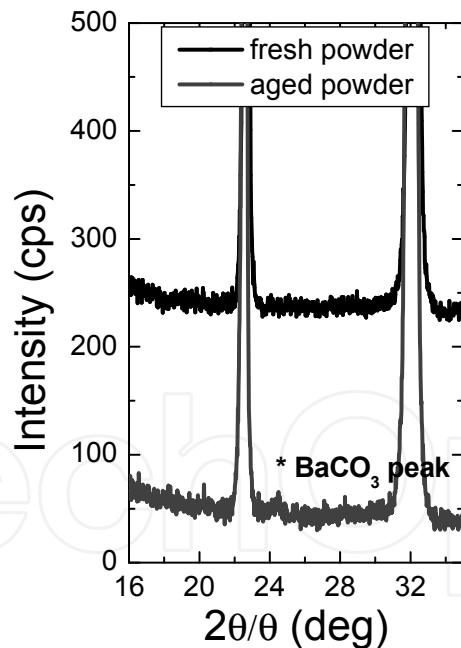Fig. 22. XRD profiles of BST raw and thermally treated powders



Fig. 23. XRD profiles of 900°C treated powder immediately after treatment and after one year

The XRD profiles of the as-received and 800 and 900°C thermally treated powders show that the crystallinity is retained in all films. However, a closer observation of the XRD pattern near 2theta=24° revealed the presence of an additional peak that can be assigned to the orthorhombic $BaCO_3$ phase (figure 22). Since the concentraton of $BaCO_3$ second phase is

high enough to surpass the sensitivity limit of the X-ray diffraction system, it can be also assumed that a peak related to this phase will also appear in XPS results. On this ground, it has been assumed that the $BaCO_3$ second phase will be responsible for the appearance of a relatively high intensity peak in the C 1s XPS peak profile of the BST60 powder, peak that should be located near 289 eV.

This is another reason for linking the peak located at 288.45 eV in C 1s XPS profile to the C state in $CO_3^{2-}$ of the $BaCO_3$ second phase. It should be notted that for powders thermally treated at $900^0C$ for 1 h, peaks generated by the presence of the second carbonate phase were not observed in the XRD profile, suggesting that this temperature is suitable for the removal of the secondary phase in the BST60 powders. To further test the BST powder instability against humidity and $CO_2$ in air some treated powder was intentionally placed in atmospheric conditions for 1 year. In figure 23, the XRD patterns near 2theta=$24^0$ are shown for freshly treated powder and powder aged in air for 1 year away from dust. The carbonate peak becomes visible again suggesting that humidity and $CO_2$ from air were sufficient to trigger $Ba^{2+}$ ion removal from BST60 powders and formation of $BaCO_3$ in the outershell of BST particles.

The effect of powder thermal treatment on the physical and electrical properties of the AD-fabricated BST60 films was also analyzed. As shown in figure 24, the dielectric constant of AD-fabricated films using $900^0C$ treated powders is highest among the investigated films being close to 200 for a wide frequency range. The dielectric loss in all samples was below 0.06 and no marked changes in this parameter were observed. Since the grain size is similar in all the films, the difference in dielectric constant is not due to its dependence on grain size.
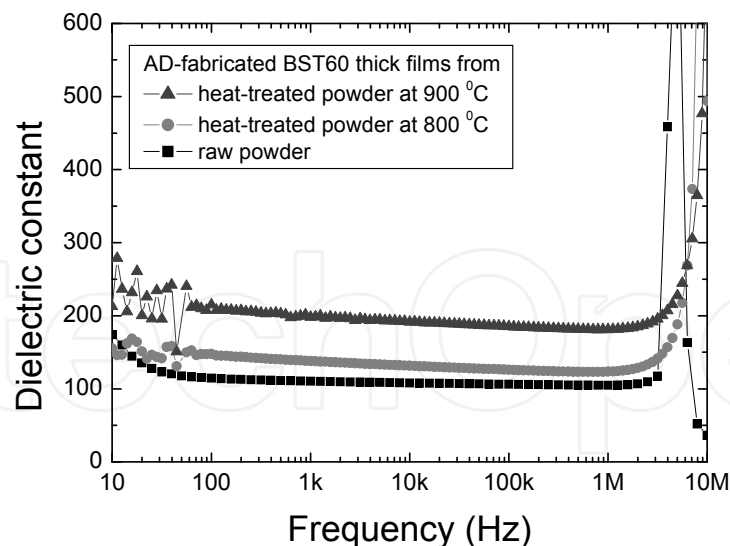


Fig. 24. Frequency dependence of dielectric constant for AD BST thick films deposited from raw and thermally treated powders

Due to the unique way deposition of films take place in AD, the material in the outershell of the crystalline particles participating in the consolidation process will always be found to form grain boundaries in the as-deposited AD films. The increase in dielectric constant can

be correlated with the improvement of the grain boundary regions since, by minimizing the ammount of the secondary phase, the low dielectric constant carbonate phase will be less present at the grain boundary. Moreover, the leakage in AD films is improved by annealing the powder at 900$^0$C (figure 24).
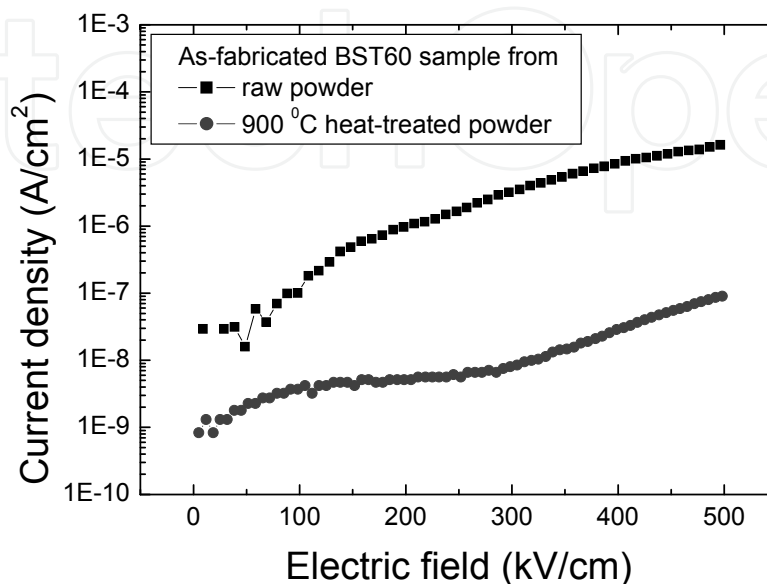


Fig. 25. Leakage of BST films deposited from raw and 900$^0$C thermally treated powders

For the AD-fabricated BST60 thick films obtained from 900$^0$C treated powders, the leakage currents stay below $10^{-7}$ A/cm$^2$ for applied electric fields up to 500 kV/cm. A reduction in leakage current of one or two orders of magnitude is observed for the AD-fabricated films obtained from 900$^0$C treated powders as compared with the films fabricated from raw powders. This is another indication that the grain boundaries of the BST60 films were modified following the thermal treatment of the powders at 900$^0$C prior to deposition. The removal of the secondary phase from the grain boundary regions by thermally treating the powder at 900$^0$C increases the resistivity of the grain boundary regions, reducing the leakage currents through the grain boundary.

Thermal treatment of commercially available BST powder at 900$^0$C is a good approach to increase the overall performance of the AD-fabricated BST thick films deposited at room temperature and to make them more attractive for embedded multilayer capacitor applications.

## 4. Conclusions

BT-based materials represent a class of materials with a wide range of applications. Here, we showed how substitution in A or B site can make these materials suitable for different applications. Two examples of how BT-based materials can show potential in specific applications are discussed.

Ba($Ti_{0.85}$,$Sn_{0.15}$) (BTS) ferroelectric thin films have been prepared by metal-organic decomposition (MOD) technique. Annealing and postannealing temperatures were

optimized to obtain films with suitable electrical properties for application in DB-mode of infrared sensing. Annealing at $700^0C$ has as the result the minimization of the leakage current and the dielectric loss. Also, the capacitance of a capacitor containing BTS thin film crystallized at this temperature will decrease more rapidly with an increase in film temperature than on a similar capacitor made with BTS thin films annealed at $800^0C$. Considering the results, annealing at $700^0C$ is suitable to fabricate with good properties for application to DB-mode of infrared sensing. Applying a postannealing treatment to the capacitors after top-electrode deposition can improve further the electrical properties of the BTS thin films. It has been found that, postannealing at $300^0C$ in air for 60 minutes, even if the leakage is higher than in the case of postannealing at $200^0C$, will increase the value of the temperature coefficient of dielectric constant (TCD) from 1 %/K to 5.6 %/K at $25^0C$ comparing with only 1.3 %/K for films postannealed at $200^0C$. A closer look on the leakage current behavior on BTS films postannealed in air reveals that an increase in postannealing temperature will reduce the oxygen diffusion from the air into the films that translates as higher leakage currents for samples postannealed at temperatures higher than $200^0C$ than on the samples postannealed at $200^0C$. However these values are still smaller than that of as-deposited BTS thin films. TCD values are higher for samples postannealed at $300^0C$ suggesting that some degree of oxygen deficiency in the film is needed in order to obtain satisfactory values for TCD. A close investigation regarding the importance of postannealing at $300^0C$ revealed the important role played by the oxygen vacancies to the value of TCD. Postannealing in air-free environment will not do much improvement to the electrical properties of the film except a relatively small increase in polarization observed in P-E hysteresis loops. On the other hand, postannealing in air will promote oxygen diffusion into the film and, as a result, a change in electrical properties of the dead-layer and a change in the lattice parameters of the crystalline BTS thin films. It can be observed that postannealing at $300^0C$ for 60 minutes is an important condition in order to fabricate BTS thin films suitable for DB-mode of infrared sensing. The results obtained after BTS film investigations were used in the fabrication of a simple-structures infrared sensing cell. The cell consist in a series of two capacitors, one used as reference capacitor and the other, fabricated on a membrane to reduce the thermal loss, used as detector-capacitor. After optimization of the BD operation mode (application of sinusoidal waves with a voltage amplitude of 3 to 5V and a frequency between 10Hz and 100Hz) sensing properties of the films were revealed. A stable infrared detection was possible even for objects (in this case a black body) heated at temperatures of $27^0C$. Good figures-of-merit such as voltage responsivity ($Rv$) of 0.1 KV/W and specific detectivity ($D^*$) of $3 \times 10^8$ cmHz$^{1/2}$W were also calculated making BTS material a strong candidate for application in DB-mode of infrared sensing.

$(Ba_{0.6},Sr_{0.4})TiO_3$ (BST60) thick films were fabricated on Cu substrates by Aerosol Deposition (AD) method. The quality of the raw powder has been checked and optimized in order to increase the dielectric constant of the fabricated films without the need of post-film-formation annealing procedure. Carbonate phase has been observed in the raw powders and it was successfully reduced by thermally treating the powder at $900^0C$. The AD-fabricated films obtained from the $900^0C$ treated powder show a dielectric constant of 200 being much higher that the dielectric constant of the AD-films obtained from the as-received powders. The leakage currents in the films fabricated from $900^0C$ treated powders stay below $10^{-7}$ A/cm$^2$ when the applied electric filed is less than 500 kV/cm and it is at least one order of magnitude smaller than for films obtained from as-received powders. The above

results indicate that thermally treating the powder at 900⁰C is a good way to improve the AD-fabricated BST60 thick films electrical properties. This results represent a step forward in our goal of ceramic fabrication at room temperature aiming integration into embedded multilayered ceramic capacitor structures in electronic devices.

## 4. Acknowledgment

## 5. References

Mueller, V.; Beige, H. & Abicht, H-P. (2004). Non-Debye dielectric dispersion of barium titanate stannate in the relaxor and diffuse phase-transition state. *Applied Physics Letters*, Vol. 84, Issue 8, (2004), pp. 1341-1343, ISSN 1077-3118

Lu, S.G.; Xu, Z.K. & Chen, H. (2004). Tunability and relaxor properties of ferroelectric barium stannate titanate ceramics. *Applied Physics Letters*, Vol. 85, Issue 22, (2004), pp. 5319-5321, ISSN 1077-3118

Yasuda, N.; Ohwa H. & Asano S. (1996). Dielectric Properties and Phase Transitions of $Ba(Ti_{1-x}Sn_x)O_3$ Solid Solution. *Japanese Journal of Applied Physics*, Vol. 35, (1996), pp. 5099-5103, ISSN 1347-4065

Xiaoyong, W.; Yujun, F. & Xi, Y. (2003). Dielectric relaxation behavior in barium stannate titanate ferroelectric ceramics with diffused phase transition. *Applied Physics Letters*, Vol. 83, Issue 10, (2003), pp.2031-2033, ISSN 1077-3118

Jiwei, Z.; Bo, S.; Xi, Y. & Liangying, Z. (2004). Dielectric and ferroelectric properties of $Ba(Sn_{0.15}Ti_{0.85})O_3$ thin films grown by a sol-gel process, *Materials Research Bulletin*, Vol. 39 (September 2004), pp. 1599-1606, ISSN 0025-5408

Fukuda, Y.; Haneda, H.; Sakaguchi, I.; Numata, K.; Aoki, K. & Nishimura, A. (1997). Dielectric Properties of $(Ba,Sr)TiO_3$ Thin Films and their Correlation with Oxygen Vacancy Density. *Japanese Journal of Applied Physics*, Vol 36 (1997), pp. L1514-L1516, ISSN 1347-4065

Sze, S.M. (1981). *Physics of semiconductor devices*, Wiley-Interscience, New-York, USA, ISBN 0-471-05661-8

Fukuda, Y.; Numata, K.; Aoki, K. ; Nishimura, A.; Fujihashi, G.; Okamura, S.; Ando, S. & Tsukamoto, T. (1998). Effects of Postannealing in Oxygen Ambient on Leakage Properties of $(Ba,Sr)TiO_3$ Thin-Film Capacitors. *Japanese Journal of Applied Physics*, Vol. 37 (1998), pp. L453- L455, ISSN 1347-4065

Noda, M.; Hashimoto, K.; Kubo, R.; Tanaka, H.; Mukaigawa, T.; Xu, H. & Okuyama, M. (1999), A new type of dielectric bolometer mode of detector pixel using ferroelectric thin film capacitors for infrared image sensor. *Sensors and Actuators A*, Vol. 77, (Septemper 1999), pp. 39-44, ISSN 0924-4247

Balcerak, R.S. (1999). Uncooled IR imaging: technology for the next generation. *Proceedings of the 25th SPIE Conference on Infrared Technology and Applications*, Vol. 3698, pp. 110-118, ISBN 9780819431721, Orlando, FL, USA, April 5-9, 1999

Radford, W.; Murphy, D.; Finch, A.; Hay, K.; Kennedy, A.; Ray, M.; Sayed, A.; Wyles, J.; Wyles, R. & Varesi, J. (1999). Sensitivity improvements in uncooled microbolometer FPAs. *Proceedings of the 25th SPIE Conference on Infrared Technology and Applications*, Vol. 3698, pp. 119-130, ISBN 9780819431721, Orlando, FL, USA, April 5-9, 1999

Noda, M.; Mukaigawa, T.; Hashimoto, K.; Kiyomoto, T.; Xu, H.; Kubo, R.; Tanaka, H.; Usuki, T. & Okuyama, M. (1999). Simple detector pixel of dielectric bolometer mode and its device structure for an uncooled IR image sensor. *Proceedings of the 25th SPIE Conference on Infrared Technology and Applications*, Vol. 3698, pp. 565-573, ISBN 9780819431721, Orlando, FL, USA, April 5-9, 1999

Noda, M. ; Inoue, K. ; Ogura, M. ; Xu, H. ; Murakami, S. ; Kishihara, H. & Okuyama, M. (2002). An uncooled infrared sensor of dielectric bolometer mode using a new detection technique of operation bias voltage. *Sensors and Actuators A*, Vol. 97-98, (April 2002), pp. 329-336, ISSN 0924-4247

Akedo, J. & Lebedev, M. (1999). Microstructure and Electrical Properties of Lead Zirconate Titanate ($Pb(Zr_{52}/Ti_{48})O_3$)Thick Films Deposited by Aerosol Deposition Method. *Japanese Journal of Applied Physics*, Vol. 38, (1999), pp. 5397-5401, ISSN 1347-4065

Akedo, J.; Minami, N.; Fukuda, K.; Ichiki, M. & Maeda, R. (1999). Electrical properties of direct deposited piesoelectric thick film formed by gas deposition method annealing effect of the deposited films. *Ferroelectrics*, Vol. 231 (1999), pp. 285-292, ISSN 1563-5112

Akedo, J. & Lebedev, M. (2001). Influence of Carrier Gas Conditions on Electrical and Optical Properties of $Pb(Zr,Ti)O_3$ Thin Films Prepared by Aerosol Deposition Method. *Japanese Journal of Appied. Physics*, Vol. 40, (2001), pp. 5528-5532, ISSN 1347-4065

Akedo, J. (2004). Aerosol Deposition Method for Fabrication of Nano Crystal Ceramic Layer, *Materials Science Forum*, Vol. 449-452, (2004), pp. 43-48, ISSN 1662-9752

Akedo, J. (2006). Aerosol Deposition of Ceramic Thick Films at Room Temperature: Densification Mechanism of Ceramic Layers. *Journal of the American Ceramic Society*, Vol. 89, Issue 6, (June 2006), pp. 1834-1839, ISSN 1551-2916

Kirchoefer, S.W. ; Cukauskas, E.J.; Barker, N.S.; Newman, H.S. & Chang, W. (2002). Barium-strontium-titanate thin films for application in radio-frequency-microelectromechanical capacitive switches. *Applied Physics Letters*, Vol. 80, Issue 7, (2002), pp. 1255-1257, ISSN 1077-3118

Acikel, B.; Taylor, T.R.; Hansen, P.J.; Speck, J.S. & York, R.A. (2002). A new high performance phase shifter using $Ba_xSr_{1-x}TiO_3$ thin films. *IEEE Microwave and Wireless Components Letters*, Vol. 12, Issue 7, (2002), pp. 237-239, ISSN 1531-1309

Hwang, C.S; Park, S.O.; Cho, H.J.; Kang, C.S.; Lee S.I.; & Lee, M.Y. (1995). Deposition of extremely thin $(Ba,Sr)TiO_3$ thin films for ultra-large-scale integrated dynamic random access memory application. *Applied Physics Letters*, Vol. 67, Issue 19, (1995), pp. 2819-2821, ISSN 1077-3118

Zhu, H.; Miao, J.; Noda, M. & Okuyama, M. (2004). Preparation of BST ferroelectric thin film by metal organic decomposition for infrared sensor. *Sensors and Actuators A*, Vol. 110, Issues 1-3, (February 2004), pp. 371-377, ISSN 0924-4247

Tissot, J.L. (2003). Uncooled focal plane infrared detectors: the state of the art (in French). *Comptes Rendus Physique*, Vol. 4, Issue 10, ( December 2003), pp. 1083-1088, ISSN 1631-0705

Popovici, D.; Tsuda, H. & Akedo, J. (2009). Postdeposition annealing effect on (Ba0.6,Sr0.4)TiO3 thick films deposited by aerosol deposition method. *Journal of Applied Physics*, Vol. 105, Issue 6, (March 2009), pp. 061638-1-061638-5, ISSN 1089-7550

Popovici, D.; Tsuda, H. & Akedo, J. (2008). Fabrication of $(Ba_{0.6},Sr_{0.4})TiO_3$ Thick Films by Aerosol Deposition Method for Application to Embedded Multilayered Capacitor Structures. *Japanese Journal of Applied Physics*, Vol. 47, (September 2008), pp. 7490-7493, ISSN 1347-4065

Hennings, D. & Mayr, W. (1978), Thermal decomposition of (BaTi) citrates into barium titanate. *Journal of Solid State Chemistry*, Vol. 26, Issue 4, (December 1978), pp. 329-338, ISSN 0022-4596

Coutures, J.P.; Odier, P. & Proust, C. (1992). Barium titanate formation by organic resisns formed with mixed citrate. *Journal of Materials Science*, Vol. 27, No. 7, (1992), pp. 1849-1856, ISSN 1573-4803

Hennings, D. & Schreinemacher, S. (1992). Characterization of hydrothermal barium titanate. *Journal of European Ceramic Society*, Vol. 9, Issue 1, (1992), pp. 41-46, ISSN 0955-2219

Stockenhuber, M.; Mayer, H. &. Lercher, J.A (1993). Preparation of Barium Titanates from Oxalates. *Journal of American Ceramic Society*, Vol. 76, Issue 5, (May 1993), pp. 1185-1190, ISSN 1551-2916

Lemoine, C.; Gilbert, B.; Michaux, B.; Pirard, J.P. & Lecloux, A.J. (1994). Synthesis of barium titanate by the sol-gel process. *Journal of Non-Crystalline Solids*, Vol. 175, Issue 1, (September 1994), pp. 1-13, ISSN 0022-3093

Ries, A.; Simoes, A.Z.; Cilense, M.; Zaghete, M.A. & Varela, J.A. (2003). Barium strontium titanate powder optained by polymeric precursor method. *Materials Characterization*, Vol. 50, Issues2-3, (March 2003), pp. 217-221, ISSN 1044-5803

Lencka, M.M. & Riman, R.E. (1993). Thermodynamic modeling of hydrothermal synthesis of ceramic powders. *Chemistry of Materials*, Vol 5, Issue 1, (January 1993), pp. 61-70, ISSN 1520-5002

Abicht, H.-P.; Voltzke, D.; Roder, A.; Schneider, R. & Voltersdorf, J. (1997). The influence of the milling liquid on the properties of barium titanate powders and ceramics. *Journal of Materials Chemistry*, Vol. 7, Issue 3 (1997), pp. 487-492, ISSN 1364-5501

Voltzke, D.; Gablenz, S.; Abicht, H.-P.; Schneider, R.; Pippel, E. & Woltersdorf, J. (1999). Surface modification of barium titanate powder particles. *Materials Chemistry and Physics*, Vol. 61, Issue 2, (October 1999), pp. 110-116, ISSN 0254-0584.

M. Viviani, M.; Buscaglia, M.T.;. Nanni, P; Parodi, R.; Gemme, G. & Dacca, A. (1999). XPS investigation of surface properties of $Ba_{(1-x)}Sr_xTiO_3$ powders prepared by low temperature aqueous synthesis. *Journal of the European Ceramic Society*, Vol.19, Issues 6-7, (June 1999), pp. 1047-1051, ISSN 0955-2219

Wagner, C.D.; Riggs, W.M.; Davis, L.E. & J.F. Moulder, J.F. (1979). *Handbook of X-ray photoelectron spectroscopy*, ed. G.E. Muilenberg (Perkin-Elmer Corporation, Physical Electronics Division 1979), p.38
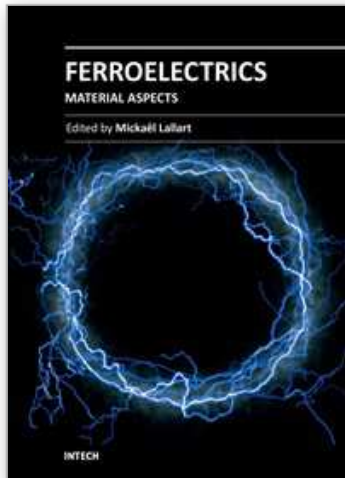
**Ferroelectrics - Material Aspects**

Edited by Dr. Mickaël Lallart

Ferroelectric materials have been and still are widely used in many applications, that have moved from sonar towards breakthrough technologies such as memories or optical devices. This book is a part of a four volume collection (covering material aspects, physical effects, characterization and modeling, and applications) and focuses on ways to obtain high-quality materials exhibiting large ferroelectric activity. The book covers the aspect of material synthesis and growth, doping and composites, lead-free devices, and thin film synthesis. The aim of this book is to provide an up-to-date review of recent scientific findings and recent advances in the field of ferroelectric materials, allowing a deep understanding of the material aspects of ferroelectricity.

**How to reference**

In order to correctly reference this scholarly work, feel free to copy and paste the following:

Daniel Popovici, Masanori Okuyama and Jun Akedo (2011). Barium Titanate-Based Materials – a Window of Application Opportunities, Ferroelectrics - Material Aspects, Dr. Mickaël Lallart (Ed.), ISBN: 978-953-307-332-3, InTech, Available from: http://www.intechopen.com/books/ferroelectrics-material-aspects/barium-titanate-based-materials-a-window-of-application-opportunities

# INTECH
open science | open minds